Tuning FlaSh: Redesign of the Dynamics, Voltage Range, and Color of the Genetically Encoded Optical Sensor of Membrane Potential

Giovanna Guerrero, Micah S. Siegel, Botond Roska, Eli Loots, and Ehud Y. Isacoff
Department of Molecular and Cell Biology, University of California, Berkeley, Berkeley, California 94720-3200, USA

ABSTRACT The optical voltage sensor FlaSh, made from a fusion of a GFP "reporter domain" and a voltage-gated *Shaker* K^+ channel "detector domain," has been mutagenically tuned in both the GFP reporter and channel detector domains. This has produced sensors with improved folding at 37°C, enabling use in mammalian preparations, and yielded variants with distinct spectra, kinetics, and voltage dependence, thus expanding the types of electrical signals that can be detected. The optical readout of FlaSh has also been expanded from single wavelength fluorescence intensity changes to dual wavelength measurements based on both voltage-dependent spectral shifts and changes in FRET. Different versions of FlaSh can now be chosen to optimize the detection of either action potentials or synaptic potentials, to follow high versus low rates of activity, and to best reflect electrical activity in cell types with distinct voltages of operation.

INTRODUCTION

Electrical waves represent one of the fundamental modalities of signaling in the nervous system. Although electrophysiological methods have provided vast insight as to how individual or small groups of neurons process information, a direct view of how a neural circuit operates as an ensemble has been hard to obtain. Better suited to capture with high spatial and kinetic resolution how activity flows through neuronal circuits are methods that rely on imaging of either intrinsic optical signals, which occur from voltage-induced changes in membrane birefringence, or changes in absorbance or fluorescence of voltage-sensitive or calcium-sensitive organic dyes. However, the advantages of high kinetic and spatial resolution of the established methods of optical imaging are offset by several shortcomings. First, birefringence and fluorescent dye methods usually detect signals indiscriminately from neurons and non-neuronal cells, such as glia, which represent a large fraction of the total membrane surface in brain, and therefore a major component of the signal. Second, the methods do not distinguish between types of neurons, as can be done from functional identification in single cell recordings.

A potential solution to these limitations has emerged with the generation of genetically encoded, protein-based optical sensors, which can be placed under control of cell-specific promoters and even targeted to subcellular compartments where specific signals dominate (e.g., dendrites for synaptic potentials and axons for action potentials). These sensors, which use the Green Fluorescent Protein (GFP) as a reporter of cellular signaling, have permitted the detection of Ca^{2+}, Zn^{2+}, pH, Cl^-, and voltage (Miyawaki et al., 1997; Baird et al., 1999; Miesenbock et al., 1998; Kneen et al., 1998; Llopis et al., 1998; Jayaraman et al., 2000; Siegel and Isacoff, 1997; Romoser et al., 1997; Nagai et al., 2000; Pearce et al., 2000; Sakai et al., 2001; Ataka and Pieribone, 2002).

In addition to solving the problem of targeting, genetically encoded sensors afford an additional advantage: it should be possible to "rationally tune" protein sensors by modification of their functional domains with mutations that are known to adjust their kinetics or dynamic range of operation. Such a modulation has already been accomplished for Cameleon, a construct in which two GFPs are linked by a calmodulin-M13 fusion peptide (Miyawaki et al., 1997). When Ca^{2+} binds to calmodulin a structural rearrangement in the linker changes the interaction between the GFPs, producing a change in fluorescence resonance energy transfer (FRET). Mutating Ca^{2+} binding sites in calmodulin reduces the sensitivity of Cameleon for Ca^{2+} in a predicted manner (Miyawaki et al., 1997).

Here we report the kinetic, dynamic range and color tuning of our voltage-sensing optical sensor FlaSh (Fluorescent *Shaker*), a fusion between the voltage-gated *Shaker* K^+ channel and a C-terminal deleted GFP (Siegel and Isacoff, 1997). This chimera had previously been shown to couple the voltage-dependent rearrangements of the *Shaker* channel to the fluorescence emission of a GFP. By modifying the GFP reporter, we have produced sensors with improved folding at 37°C, and with distinct spectra. Sensors of different colors can be targeted to different cell types to enable the synchronous measure of activity from two or three subpopulations of intermingled cells in the same neural circuit, which could not be otherwise distinguished. We also describe versions of FlaSh that are improved for the detection of action potentials, on one hand, or synaptic potentials, on the other, and that are adapted for cell types with distinct voltages of operation. Finally, we expand our optical readout from single wavelength fluorescence intensity changes to dual wavelength measurements based on

Submitted May 8, 2002, and accepted for publication July 19, 2002.

Address reprint requests to Ehud Y. Isacoff, Department of Molecular and Cell Biology, University of California, Berkeley, 271 LSA, MC 3200, Berkeley, CA 94720-3200. Tel.: 510-642-9853; Fax: 510-642-4968; E-mail: eisacoff@socrates.berkeley.edu.

0006-3495/02/12/3607/12 $2.00

spectral shifts and FRET, thus enabling elimination of movement artifacts and changes in probe quantity or concentration, and augmenting the fractional signal change.

MATERIALS AND METHODS

Construction of FlaSh variants

The versions of GFP used—eGFP, GFPuv, eCFP, and eYFP (Clontech, Palo Alto, CA) and Ecliptic GFP (kindly provided by Dr. James Rothman)—were cloned into both W434F and W434, inactivation ball (−ball) removed (Δ6–46; 11) ShH4, into the same position as before (Siegel and Isacoff, 1997), using the same primers. An *Rsr*II–*Bsm*I fragment of ShH4 L366A (kindly provided by Dr. Richard Aldrich), which flanks the point mutation, was inserted into FlaSh wtGFP to make L366A FlaSh. All FlaSh cDNAs were transcribed using Megascript T7 (Ambion, Austin, TX) with a 4:1 methyl CAP/rGTP ratio, and the precipitated cRNA was resuspended in ultrapure water for injection. All other aspects of oocyte isolation, injection, and incubation were as described previously (Isacoff et al., 1990).

Voltage-clamp fluorimetry and analysis

Two-electrode voltage clamping was performed with a Dagan CA-1B amplifier (Dagan Corporation, Minneapolis, MN). An HC120-05 photomultiplier (Hamamatsu, Bridgewater, NJ) was used for fluorescence measurements on a Nikon TMD inverted microscope. Data were sampled with a Digidata 1200 AE interface (Axon Instruments, Foster City, CA) at 5 KHz and low-pass filtered at 1 KHz with an 8-pole Bessel filter (Frequency Devices, Haverhill, MA). Acquisition and analysis of data were done with Axon Instruments pClamp8. Samples were illuminated with a 100 W mercury arc lamp. The filter sets used were from Chroma Technology, Brattleboro, VT. Fluorescence traces were digitally filtered, primarily for aesthetic purposes, to 100 Hz with a Gaussian function where indicated. External solution for all recordings consisted of 110 mM NMG, 2 mM CaMES, and 10 mM Hepes (pH 7.5). Oocytes were clamped to −80 mV in all experiments except for experiments with Flash L366A, which were performed at a −100 mV holding potential. Voltage waveforms in Fig. 7 and 8 have been described before (Roska et al., 1998).

Filter sets

The following filter combinations were used. For FRET, eGFP, Ecliptic, eCFP, wtGFP, and GFPuv: Ex. 425–475, D. 480LP, Em. 485–535. For eGFP, eYFP, and wtGFP: Ex. 460–500, D. 505LP, Em. 510–560.

RESULTS

In tuning FlaSh we made mutations in both the "detector" protein—the voltage-dependent *Shaker* K^+ channel—and in the reporter protein, GFP. We preserved the original architecture of FlaSh (Siegel and Isacoff, 1997), with GFP deleted for its last six amino acids from the C-terminal end (GFP (Δ233–238)) inserted into the *Shaker* K^+ channel near the internal end of the sixth transmembrane domain (Fig. 1). As before, we used the W434F mutation of *Shaker* (*Shaker* (W434F)), which locks the channel in a nonconducting conformation (Perozo et al., 1993), thus preventing the sensor protein from contributing ionic currents to the cell. However, a version of FlaSh in a conducting *Shaker* background was used in one experiment to try to identify functional rearrangements that evoke changes in fluorescence (ΔF) of GFP (Fig. 2). The constructs were characterized with voltage-clamp fluorometry (Mannuzzu et al., 1996) in *Xenopus* oocytes, where they form homotetramers, each channel thus containing four GFPs.

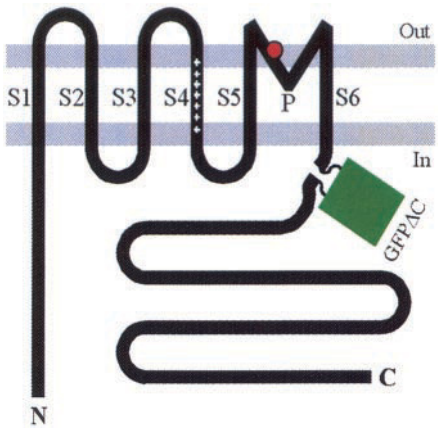

FIGURE 1 The FlaSh construct. Membrane topology model of FlaSh shows the six transmembrane domains of the *Shaker* channel, including the charged voltage sensing S4. GFP is fused in-frame in the C-terminal domain of the voltage-gated *Shaker* K^+ channel, 25 amino acids away from the internal end of S6, at a location where conformational rearrangements in the channel perturb the fluorescence of GFP. The GFP has been sensitized to the rearrangements of the channel by deletion of the last eight residues in the C-terminal, which are disordered in the crystal structure (Patterson et al., 1997).

Functional rearrangements in the *Shaker* channel that evoke fluorescence responses in GFP

The original FlaSh, which contains wild-type GFP (FlaSh (wtGFP)), undergoes a three-phase fluorescence change (ΔF): a small, fast transient fluorescence *increase* (τ = 13.7 ± 0.4 ms) is followed by larger intermediate (τ = 85.3 ± 10.0 ms) and late phases (τ = 137.0 ± 7.2 ms) of fluorescence *decrease* in response to a step of depolarization (Fig. 2). We previously established that changes in GFP emission were directly coupled to gating rearrangements of *Shaker* (W434F), and not to changes in pH or to GFP rearrangements induced by voltage (Siegel and Isacoff, 1997). To look at the relation of the fluorescent change to current activation, we inserted wtGFP at the same site in conducting (W434) N-ball deleted channels. In the conducting channel, the upward transient ΔF was found to turn on with the turning on of the ionic current. In the nonconducting (W434F) channel, which has its inactivation gate locked shut, this upward transient ΔF turned on with the late phase of gating charge movement, which is tightly coupled to channel opening (Schoppa and Sigworth, 1998). This behavior is consistent with GFP sensing a structural rearrangement that activates or opens the activation gate of the

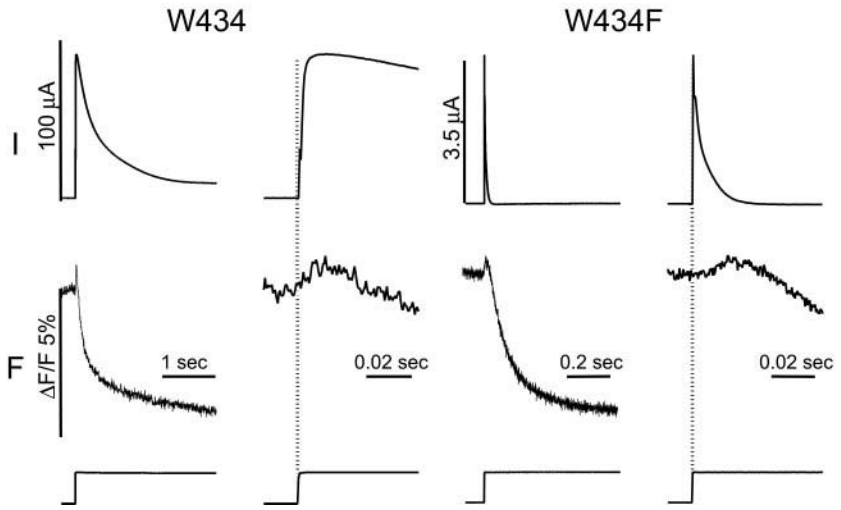

FIGURE 2 Relationship between the phases of the ΔF and the gating rearrangements of FlaSh (wtGFP). Fluorescence (F) is measured in parallel with current (I). The wild-type conducting N-type inactivation ball-deleted ($\Delta 6-46$) (W434) channel opens its activation gate rapidly in response to a depolarizing step from −80 to 0 mV and conducts ionic current, which declines as the slow inactivation gate closes. An early upward ΔF rises in parallel with the rise in the ionic current and with the second phase of the gating current, suggesting that wtGFP responds to the channel rearrangement that activates the channel or opens the activation gate. Two additional downward ΔF components have intermediate and late kinetics. The intermediate component is faster and the late component slower than the inactivation of the W434 ionic current (i.e., closure of the inactivation gate), and these components persist in W434F, when the inactivation gate is shut (Fig. 3 and Siegel and Isacoff, 1997). Traces displayed at two sweep speeds, as indicated. Responses are to a single maintained voltage step between −80 mV and +40 mV. Traces are the average of 10 sweeps.

channel. The intermediate and late components of the downward ΔF were, respectively, faster and slower than the slow inactivation of the W434 ionic current (Fig. 2). These components persisted, albeit with faster kinetics, when the inactivation gate was permanently shut by the W434F mutation (Fig. 2), suggesting that they are related to inactivation, but not caused by the gating step itself. Further experiments will be needed to better define these steps. We found that excitation at longer wavelengths evoked a response that virtually lacked the early upward ΔF transient (Fig. 3, wtGFP, *arrow*), but preserved the intermediate and late components. This suggests that the protonated state of the GFP chromophore, which has the excitation peak at ~395 nm (Patterson et al., 1997), is

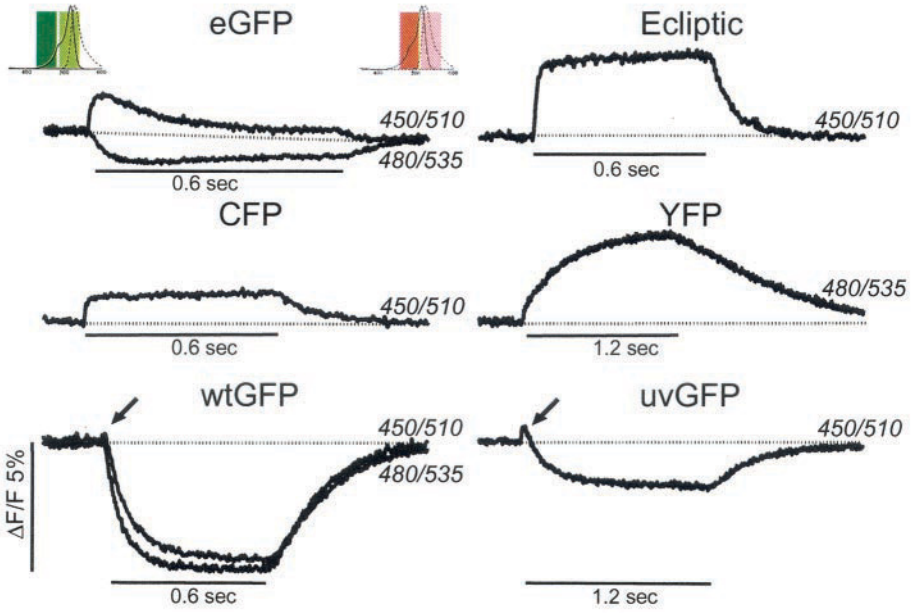

FIGURE 3 Distinct polarity and kinetics of fluorescence response of six variant GFPs in the FlaSh construct. Variant GFPs in FlaSh (see text and Table 1 for GFP mutations and taus) have various degrees of prominence of early, intermediate, and late components of ΔF. Response to a depolarizing step (−80 to 0 mV for duration of time bar) is shown for optimal excitation and emission wavelengths. Where other excitation and emission wavelengths gave different responses (rather than simply smaller ones), these are shown (eGFP and wtGFP). Filters: *450/510* = 425–475ex, 480D, 485– 535em; *480/535* = 460–500ex, 505D, 510–560em. Arrow indicates early upward ΔF in wtGFP and GFPuv, which we attribute to a decrease in self-quenching.

TABLE 1 Summary of FlaSh variants and their fluorescence on and off kinetics in response to depolarizing steps

FlaSh Variant	Mutations	Optical Filter Sets	Fluorescence Time Constants (ms)
FlaSh (wtGFP)	Channel: W434F GFP:(Δ233–238)	450/25X, D480LP, 510/25M	$\tau_1 = 13.7 \pm 0.4$ $\tau_2 = 85.3 \pm 10.0$ $\tau_3 = 37.0 \pm 7.2$ $\tau_{off} = 60.1 \pm 12.0$ $\tau_{pulse\ on} = 18.5 \pm 1.8$
		480/20X, D505LP, 535/25M	$\tau_1 = 56.5 \pm 0.4$ $\tau_2 = 102.5 \pm 1.1$ $\tau_{off} = 173.7 \pm 1.4$
FlaSh (GFPuv)	Channel: W434F GFP:F99S, M153T, V163A, (Δ233–238)	450/25X, D480LP, 510/25M	$\tau_1 = 11.7 \pm 0.7$ $\tau_2 = 82.4 \pm 6.5$ $\tau_3 = 176.7 \pm 15$ $\tau_{off} = 332.4 \pm 31.6$
FlaSh (Ecliptic GFP)	Channel: W434F GFP: S147D, N149Q, T161I, S202F, Q204T, A206T, (Δ233–238)	450/25X, D480LP, 510/25M	$\tau_{on} = 11.5 \pm 0.6$ $\tau_{off} = 72.5 \pm 2.3$
FlaSh (CFP)	Channel: W434F CFP: F64L, S65T, Y66W, R80Q, N146I, M153T, V163A, N164H, H231L, (Δ233–238)	450/25X, D480LP, 510/25M	$\tau_1 = 10.0 \pm 0.3$ $\tau_{off1} = 51.2 \pm 1.5$ $\tau_{off2} = 215.6 \pm 11.6$
FlaSh (eGFP)	Channel: W434F GFP:F64L, S65T, R80Q, H231L, (Δ233–238)	450/25X, D480LP, 510/25M	$\tau_1 = 18.6 \pm 0.6$ $\tau_2 = 186.3 \pm 3.6$
		480/20X, D505LP, 535/25M	$\tau_1 = 33.4 \pm 6.1$ $\tau_2 = 144.0 \pm 7.2$
FlaSh (YFP)	Channel: W434F YFP: S65G, V68L, S72A, R80Q, T203Y, H231L, (Δ233–238)	480/20X, D505LP, 535/25M	$\tau_1 = 30.0 \pm 6.1$ $\tau_2 = 367.6 \pm 6.3$
FlaSh IR (wtGFP)	Channel: (Δ6–46) GFP: (Δ233–238)	450/25X, D480LP, 510/25M	$\tau_1 = 15.7 \pm 1.1$ $\tau_2 = 58.3 \pm 1.2$ $\tau_3 = 443.8 \pm 3.1$ $\tau_{off} = 177.2 \pm 1.2$ $\tau_{pulse\ on} = 9.7 \pm 0.5$
FlaSh L366A (wtGFP)	Channel: (Δ6–46, L366A) GFP: (Δ233–238)	450/25X, D480LP, 510/25M	$\tau_1 = 11.8 \pm 1.1$ $\tau_2 = 79.0 \pm 3.8$ $\tau_3 = 124.3 \pm 8.1$ $\tau_{off} = 206.4 \pm 10.1$
FlaSh (CFP) + FlaSh (YFP) Conjection	See mutations for each individual variant	450/25X, D480LP, 535/25M	$\tau_1 = 20.2 \pm 2.1$ $\tau_2 = 248.2 \pm 7.3$ $\tau_{off} = 101.9 \pm 8.1$

X = exciter, D = dichroic, M = emitter.

more sensitive to the rearrangement that opens the channel's activation gate.

Modifying GFP yields temperature-stable spectral variants with distinct fluorescence responses to voltage

We made mutations in the wtGFP (Δ233–238) of the nonconducting version of FlaSh (carrying the *Shaker* mutation W434F) to change it in known ways to spectral variants described by others. Each of the new versions of GFP that we tested has enhanced folding at 37°C. Table 1 summarizes channel and GFP mutations for all constructs tested, as well as their resulting fluorescence kinetics. We tested one GFP that had mutations only in amino acids implicated in the thermal sensitivity of folding. The triple mutation F99S, M153T, V163A to GFPuv has been shown to leave unchanged the excitation and emission spectra (Crameri et al., 1996). As with FlaSh (wtGFP), FlaSh (GFPuv) had an upward early transient that was followed by a sustained slow downward ΔF (Fig. 3).

Ecliptic GFP (S147D, N149Q, T161I, S202F, Q204T, A206T) also preserves the 400 and 475 nm excitation peaks of wtGFP. In addition, as with wtGFP, the brightness of Ecliptic GFP decreases at lower pH across the excitation spectrum, but the sensitivity of Ecliptic GFP to pH is greater (Miesenbock et al., 1998). When excited with 425–475 nm, which mainly excites the 400 nm excitation peak (Miesen-

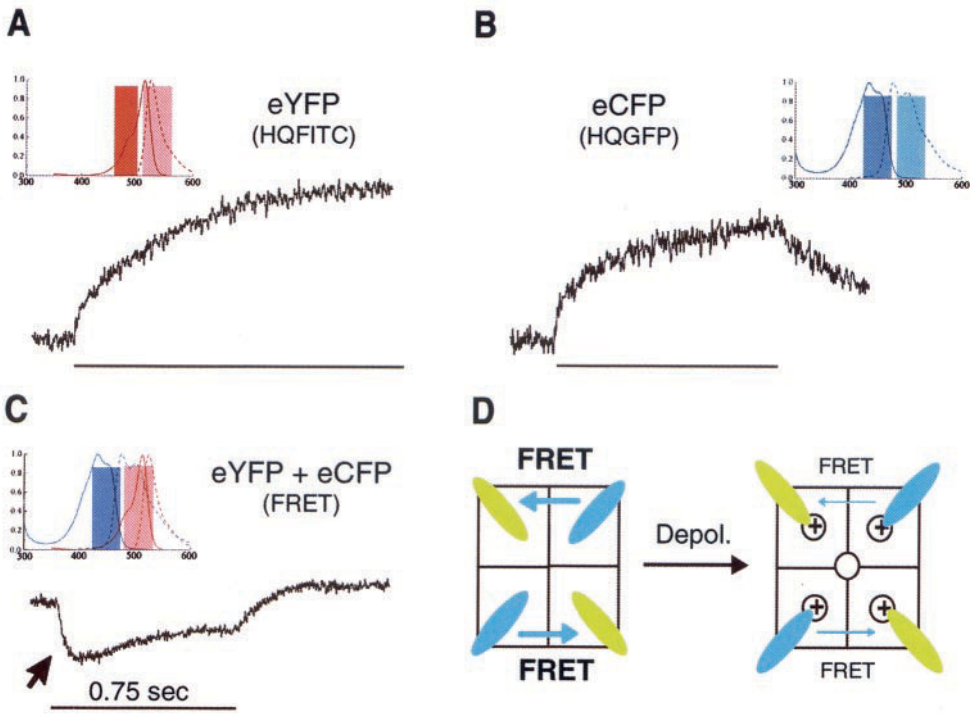

FIGURE 4 Decrease in FRET during the early part of fluorescence response to voltage. FlaSh (CFP) (*A*) and FlaSh (YFP) (*B*) have small *upward* ΔF values. (C) FlaSh (CFP+YFP) channels co-assembled from a 1:1 mixture of FlaSh (CFP) and FlaSh (YFP) subunits have a large ΔF, with an initial *downward* component followed by a slow *upward* component. The novel *downward* component, which is not present in homotetramers of either FlaSh (CFP) or FlaSh (YFP), represents a decrease in FRET. The late *upward* ΔF and overshoot in the recovery after the end of the step are consistent with the responses of FlaSh (CFP) and FlaSh (YFP) homotetramers. (*A–C*) Insets show excitation (*solid line*) and emission (*dashed line*) spectra and excitation and emission filters (*bars*) for each recording. (*D*) Cartoon of the tetrameric FlaSh (CFP+YFP) channel showing one possible subunit order for the 2:2 CFP/YFP stoichiometry (the most prevalent stoichiometry in the mix) in which the CFPs are diagonally located with respect to the YFPs. An early rearrangement is proposed to decrease the FRET from CFP on one subunit to YFP on another subunit, either because of an increase in distance (as shown) or a change in relative dipole orientation (not shown), both of which decrease electronic coupling.

back et al., 1998 and spectral panel in Fig. 3), FlaSh (Ecliptic GFP) had a monotonic fluorescent onset and decay (τ_{on} = 11.5 ± 0.6 ms, τ_{off} = 72.5 ± 2.3 ms), both of which were faster than FlaSh (wtGFP) (τ_{on} = 85.3 ± 10.0 ms; τ_{off} = 160.1 ± 12.0 ms) (Fig. 3). The fractional ΔF of FlaSh (Ecliptic GFP) was reduced (86% of maximal ΔF), but not changed in character upon excitation with at 460–500 nm light, which mainly excites the 475 nm peak (data not shown).

Each of the three remaining versions of GFP that were examined—eCFP (F64L, S65T, Y66W, R80Q, N146I, M153T, V163A, N164H, H231L), eGFP (F64L, S65T, R80Q, H231L), and eYFP (S65G, V68L, S72A, R80Q, T203Y, H231L)—have their excitation peaks shifted to longer wavelengths, with major peaks at 434, 489, and 514 nm, respectively (Patterson et al., 1997; Heim and Tsien, 1996; Ormo et al., 1996). The ΔF of FlaSh (CFP) had a fast upward ΔF followed by a slow upward ΔF (Fig. 3), while FlaSh YFP (Figs. 3 and 4 *A*) had only a small fast component (τ = 30.0 ± 6.1 ms) and a large slow component (τ = 367.6 ± 6.3 ms). FlaSh (CFP) and FlaSh (YFP) did not change in polarity or kinetics of the ΔF with shorter wavelength excitation (data not shown). In contrast, the polarity of the ΔF of FlaSh (eGFP) was reversed when switching from excitation of the main longer wavelength peak (*downward* fast component, followed by *upward* slow component) to excitation of the shorter wavelength shoulder (*upward* fast component, followed by *downward* slow component) at 425–475 nm and 460–500 nm, respectively. While the $\Delta F/F$ of FlaSh (eGFP) was smaller than that of the others, this FlaSh version has the advantage of a ratiometric measure at both excitation wavelengths.

A FRET readout from FlaSh

A second form of ratiometric measure that we attempted involved FRET between CFP and YFP attached at the same location to different subunits of FlaSh channels. A rearrangement should change FRET efficiency if it changed the orientation of CFP on one subunit with respect to YFP on another, or if it changed the distance between the CFP and

YFP. We co-expressed FlaSh (CFP) and FlaSh (YFP) in a 1:1 ratio, which is predicted to yield a binomial distribution of stoichiometries of the four subunits, with channels containing 4C, or 3C/1Y, or 2C/2Y, or 1C/3Y, or 4Y subunits. Most of the channels (14/16) are expected to have at least one subunit of each type and thus to participate in FRET, although the relative inter-subunit distances and orientations will differ depending on whether CFP is at diagonal or neighboring positions with respect to YFP (Fig. 4 *D* illustrates a stoichiometry expected to occur in 2/16 of the channels: a channel with 2 CFP diagonally located with respect to 2 YFP subunits). We set out to measure sensitized emission from YFP indirectly excited through CFP by exciting CFP at 425–475 nm and measuring YFP emission at 485–535 nm.

FlaSh channels containing a mixture of CFP and YFP subunits had an early *downward* ΔF followed by a slow and smaller upward ΔF (Fig. 4 *C*). The slow increase in brightness of the CFP+YFP channels resembled that seen with CFP or YFP alone (Fig. 4 *A* and *B*), and we attributed it to the impact on both CFP and YFP of the channel's late inactivation rearrangement. However, the early *downward* ΔF appeared to be due to a decrease in FRET, as it was not seen in either CFP or YFP alone (Fig. 4 *A* and *B*). The channel rearrangement that decreases FRET may be either a rotation of S6 and/or an increase in distance between the internal ends of S6 (Fig. 4 *D*), both of which have been proposed to occur upon channel opening (Liu et al., 1997; Baukrowitz and Yellen, 1996; Jiang et al., 2002).

Kinetic variants of FlaSh

One of the properties of FlaSh (wtGFP) is that short impulses evoke prolonged responses, which far outlast the impulse (see Fig. 6, *top*). The stretched response facilitates the optical detection of a single impulse, but this advantage is offset by two facts: 1) it will be harder to determine the exact timing of the impulse, and 2) a small number of impulses at a modest frequency saturate the sensor, limiting its usefulness for the detection of action potential trains. Faster versions of FlaSh should increase the dynamic precision of the report and broaden the range of action potential frequency over which FlaSh can be used.

The differences in response kinetics between the GFP variants (Fig. 3) suggested that the fluorescence readout of impulse activity should also differ. We compared the impulse responses of the fastest (Ecliptic GFP) and slowest (YFP) versions of FlaSh. The impulse response of FlaSh (ecliptic GFP) rapidly rose to a substantial fraction (80%) of the maximal $\Delta F/F$ for that variant and then decayed to baseline at a slightly more quickly (τ_{off} = 51.0 ± 0.9 ms) than FlaSh (wtGFP) (τ_{off} = 106.0 ± 3.0 ms, Fig. 5 *A*). By contrast, the slowest responding FlaSh (YFP) reached a small fraction (17%) of its maximal $\Delta F/F$, and rose and decayed slowly, with much of the fluorescence response occurring after the impulse (Fig. 5 *B*). The fast

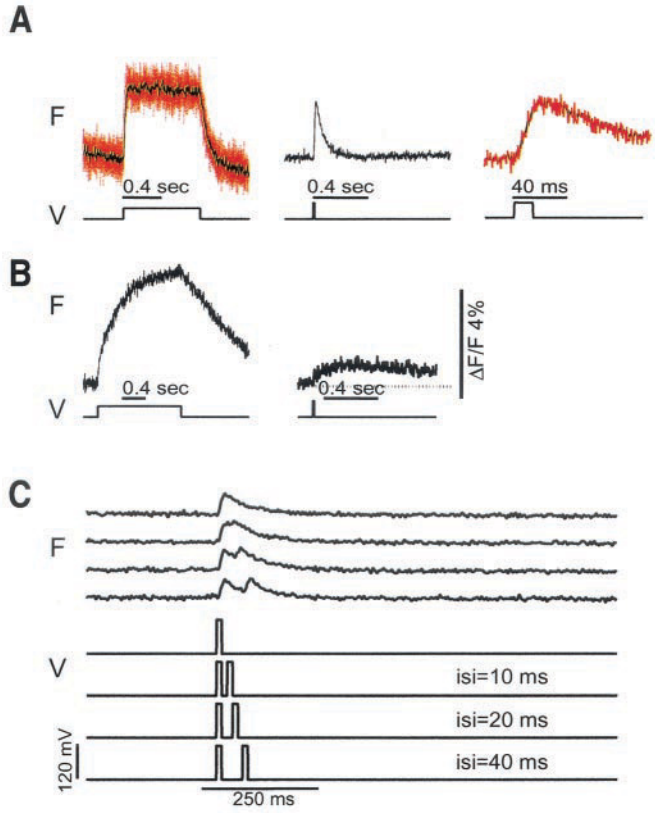

FIGURE 5 Impulse responses of fast and slow *reporter* variants of FlaSh. Comparison of step and impulse responses of (*A*) fast FlaSh (ecliptic GFP), and (*B*) slow FlaSh (YFP), variants of FlaSh that differ only in their reporter. A long depolarizing voltage step (−80 to 0 mV) evokes a rapid increase in fluorescence of FlaSh (ecliptic GFP), which is maintained for the duration of the step, and a slow saturating increase in fluorescence of FlaSh (YFP) (note different time bases). A short depolarizing impulse (−80 to +40 mV for 10 ms) evokes a short-lived large transient response from FlaSh (ecliptic GFP), which rises during the impulse almost to the full amplitude of the step response and begins to decay immediately at the end of the impulse. However, in FlaSh (YFP) an impulse evokes a response that continues to rise after the end of the step (as seen in FlaSh (wtGFP) in Fig. 6), and is only a fraction the size of the step response. (*C*) Kinetic resolution of impulse responses in FlaSh (ecliptic GFP). Fluorescence responses (*F*) to voltage impulses (V; −80 to +40 mV for 10 ms) are short enough (half-width ~30 ms) to yield resolvable responses at inter-stimulus intervals (isi) ≥20 ms.

behavior of FlaSh (ecliptic GFP) thus seems better suited than FlaSh (wtGFP) to report on neural firing with a distinct response for each action potential, while FlaSh (YFP) should act like a low-pass filter and encode firing frequency as fluorescence amplitude.

We examined the response of FlaSh (ecliptic GFP) to an impulse pair to gauge its ability to follow fast firing. Impulses given at intervals of 20 ms or longer were found to produce distinguishable responses (Fig. 5 *C*), enabling detection of individual impulses at higher rates (up to 50 Hz) than possible with FlaSh (wtGFP) (Siegel and Isacoff, 1997) and for long continuous trains of activity.

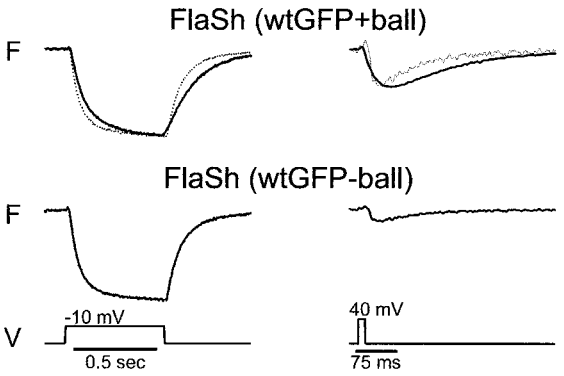

FIGURE 6 Impulse responses of fast and slow *detector* variants of FlaSh. Comparison of step and impulse responses of fast FlaSh (−ball) and slow FlaSh (+ball) variants of FlaSh (wtGFP) that differ only in their channel. A long depolarizing voltage step (−80 to 0 mV) evokes a decrease in fluorescence from both constructs. The fluorescence kinetics are faster in FlaSh (−ball). A short depolarizing impulse (−80 to +40 mV for 10 ms) evokes a large transient response from FlaSh (+ball) and a smaller and faster response from FlaSh (−ball). The response from FlaSh (−ball) begins to decay at the end of the impulse, while that of FlaSh (+ball) continues to rise after the end of the step. FlaSh (−ball) fluorescence traces have been normalized and overlayed as dashed lines on FlaSh (+ball) traces to highlight distinct kinetics.

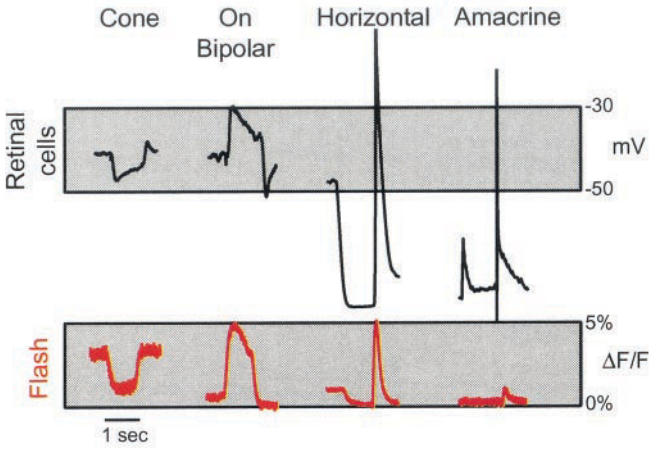

FIGURE 7 FlaSh (wtGFP) report of natural neural voltage waves. Fluorescence responses (*red traces*) of FlaSh (wtGFP) to voltage waves (*black traces*) observed in salamander retinal cones, on-bipolar cells, horizontal cells, and wide-field amacrine cells. Voltage waves were "played" to FlaSh (wtGFP) in oocytes via the voltage clamp. For each cell, the relationship between the voltage range of operation of FlaSh (wtGFP) (the dynamic range of the fluorescence-voltage relation) is shown in gray relative to the voltage wave. The poorest overlap is for the amacrine cell, for which FlaSh (wtGFP) shows the smallest response, and where the response entirely misses all of the early components of the voltage wave.

These results show that one can capitalize on the unique sensitivity to the distinct phases of channel rearrangement of each version of GFP to produce kinetic variants. However, we considered that certain versions of GFP might have desirable spectral properties that we would want to preserve in several kinetic variants. This led us to consider an orthogonal approach to kinetic tuning that would not alter the GFP reporter. We turned to modification of the detector domain of FlaSh—the *Shaker* channel—and made mutations aimed at altering the rates of those rearrangements that are sensed by GFP. We were encouraged in this approach by the observation of the difference in kinetics between FlaSh (wtGFP) in the W434 (conducting) version of the channel and the same FlaSh (wtGFP) in the W434F (nonconducting) version of the channel (Fig. 2).

Because the slow components of the fluorescence response appear to be associated with the slow inactivation of the channel (Fig. 2), mutations that alter the onset or recovery of slow inactivation are prime candidates for the rational tuning of FlaSh kinetics. We speculated that the protracted response to an impulse, where the peak of the response is reached long after the end of the impulse (Fig. 6, *top* and Fig. 5), was due to the fact that fast ball-and-chain (N-type) inactivation "immobilizes" the channel in an activated conformation for some period after the end of the impulse, protracting the opportunity for slow inactivation to occur (Lopez et al., 1991). In such a case, deletion of the N-terminal ball would be predicted to limit the onset phase of the fluorescence response to the duration of the impulse, both decreasing the amplitude of the response and shortening its duration.

As predicted, deletion of the ball gave a somewhat smaller and faster impulse response (Fig. 6, $\tau_{on} = 9.7 \pm 0.5$ ms for FlaSh without ball *vs.* $\tau_{on} = 18.5 \pm 1.8$ ms for FlaSh with ball). Both of these effects will aid in the detection of impulse trains, increasing the number and frequency of impulses that the sensor can follow before saturation.

Modifying the dynamic range of FlaSh through mutagenesis

Unlike the organic voltage-sensitive dyes, which are linear over the full range of physiological voltages (±200 mV of 0 mV), FlaSh operates over a narrow voltage range (±13 mV of −40 mV) (see Fig 8 *A*). In most neurons this narrow range should confine the FlaSh response to suprathreshold excitatory postsynaptic potentials and action potentials. In neurons with more graded potentials, such as those in the retina, the dynamic range of FlaSh coincides with some cells, but not with others (Fig. 7). To make a FlaSh sensor of subthreshold excitatory activity and inhibitory synaptic activity in typical neurons, or to adapt FlaSh to retinal neurons that operate at more negative voltages, it would be necessary to shift or reduce the steepness of the fluorescence dependence on voltage.

We examined the response of FlaSh to light-evoked voltage waves recorded in an earlier study in four types of salamander retinal cells (Roska et al., 1998). The voltage waveforms were applied via the voltage clamp to oocytes expressing FlaSh

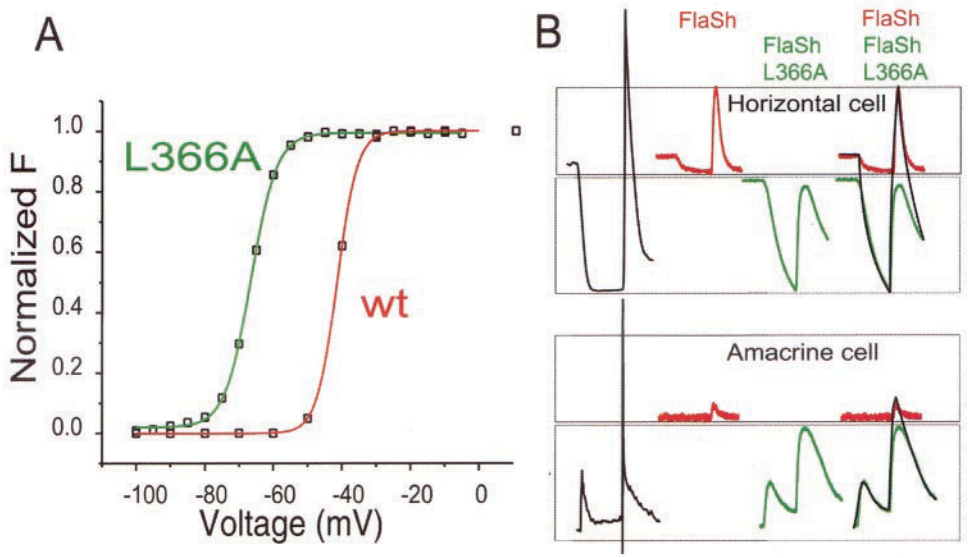

FIGURE 8 Adapting the dynamic range of FlaSh to cover natural neural signals that operate at negative voltages. (*A*) The *Shaker* S4 mutation L366A shifts the steady-state fluorescence-voltage relation by ~30 mV negative of wild-type (wt), yielding an entirely nonoverlapping dynamic range. (*B*) FlaSh (wtGFP/L366A) operates over a voltage range (*dark gray bar*) that is negative to that of FlaSh (wtGFP) (*light gray bar*), thus coinciding with different phases of the horizontal and amacrine cell voltage waves (*black traces on left*). FlaSh (wtGFP/L366A) responds more robustly to all phases of the amacrine cell voltage wave (*green traces*) than FlaSh (wtGFP) (*red traces*), and captures with different relative power the components the horizontal cell voltage wave. The arithmetically summed fluorescence signal of the two FlaSh variants (*black traces on right*) provides the best approximation to the voltage waves.

(wtGFP) (Fig. 7). FlaSh (wtGFP) fluorescence reflected reasonably well the dynamics of cone, on-bipolar cell, and horizontal cell voltage waves, even though the horizontal cell voltage range of operation is broader than that of FlaSh (wtGFP) (Fig. 7, gray band in voltage traces, *top*). However, the fluorescence response missed fast components of the wide-field amacrine cell voltage wave, which operates at voltages negative to the dynamic range of FlaSh (wtGFP).

To adapt FlaSh (wtGFP) for use in wide-field amacrine cells we made a variant of FlaSh (wtGFP) that has the *Shaker* S4 mutation L366A (Lopez et al., 1991) to shift the voltage dependence of channel gating in the negative direction. FlaSh (wtGFP/L366A) was found to have a steady-state fluorescence-voltage relation that is shifted by ~30 mV in the negative direction relative to FlaSh (wtGFP) (Fig. 8 *A*). The shift brought the sensor into the dynamic range of the amacrine cell, which now responded to all phases of the voltage wave (Fig. 8 *B*).

DISCUSSION

Fluorescent indicator dyes are essential tools for studying cellular signaling. Until recently, organic voltage-sensitive dyes were introduced into cell membranes by bath application, while organic ion indicators were introduced into cells as hydrolyzable esters or by microinjection. In both cases it has been difficult to selectively confine the dyes to large numbers of cells of a particular cell type. With the advent of protein-based indicators it has become possible, in principle, to achieve molecular targeting, to both cell type and subcellular location. The protein-based sensors developed to date use two strategies to convert physiological events into fluorescence responses in GFP. In one strategy, GFP is used as both a sensor and reporter of the physiological state of the cell, with GFP optimized to be directly sensitive to pH or halide concentration (Baird et al., 1999; Miesenbock et al., 1998; Kneen et al., 1998; Llopis et al., 1998; Jayaraman et al., 2000). In a second strategy GFP is fused to a detector peptide that changes conformation in response to an ionic, cellular, or electrical signal and induces a change in GFP fluorescence (Miyawaki et al., 1997; Baird et al., 1999; Siegel and Isacoff, 1997; Romoser et al., 1997; Pearce et al., 2000; Nagai et al., 2000; Sakai et al., 2001; Ataka and Pieribone, 2002).

A major advantage of protein-based optical sensors is that their dynamic range of operation, sensitivity to the signal (steepness of the dynamic range), kinetics of response, and spectral report by GFP can all be redesigned to optimize detection of particular signals by taking advantage of information already available in the literature about how mutations affect the function of either the detector protein or peptide or the reporter GFP. Such a strategy has already been used to reduce the calcium affinity of Cameleon, by mutating Ca^{2+} binding sites in the detector calmodulin peptide, and to produce alternative donor-acceptor pairs (Baird et al., 1999; Miyawaki et al., 1999; Mizuno et al., 2001).

We have now made spectral, kinetic, and dynamic range variants of the optical voltage sensor FlaSh through the mutation of both its reporter GFP and detector voltage-dependent *Shaker* K^+ channel. The results provide new insights into the mechanism of operation of FlaSh that suggest further avenues for tuning and for designing new optical sensors of other cellular signals.

Two limitations intrinsic to FlaSh are characterized in the study and should be pointed out here. First, although the *Shaker* channel in FlaSh is one of the fastest gating K^+ channels, it still gates more slowly than Na^+ channels, and so will not give a time accurate response to a single action potential. Second, unlike voltage-sensitive organic dyes that are linear over the entire physiological voltage range, FlaSh fluorescence has a steep sigmoidal voltage dependence and operates over a narrow voltage range. For many applications, the benefit of signal selectivity (e.g., the ability to selectively detect action potentials and exclude subthreshold potentials) may compensate for the lack of linearity and for the fact that the sensor is slower than the fastest electrical signals of a neuron. The narrowness of the dynamic range means that to obtain an optimally tuned sensor one would need a panel of variants from which to choose, switching to other variants to measure different kinds of signals. This specificity also applies to the molecular targeting of sensors to cell type and subcellular location. From the point of view of functional specificity, the straightforward nature of tuning (e.g., known mutations of the channel voltage sensor give predicted shifts in voltage dependence of reporter fluorescence) indicates that the production of a panel of sensors with distinct dynamic ranges should be as feasible as putting sensor cDNAs under the control of specific promoters.

In terms of future applications, there is a concern that FlaSh subunits can co-assemble with compatible native subunits of the Kv1 subfamily in neurons, leading to the production of a larger number of channels with faster than normal inactivation (Yang et al., 1997). Two approaches can be used to overcome this problem. First, FlaSh subunits can be linked together into a single polypeptide (Hoshi et al., 1990; Isacoff et al., 1990; Liman et al., 1992; Tytgat et al., 1993) to favor the assembly of FlaSh subunits (intra-molecular assembly) over the assembly between FlaSh and native subunits (inter-molecular assembly). Second, one can take advantage of the fact that the association of Kv1 subfamily channels with PSD-95 in neurons gives them a very slow turnover rate (Okabe et al., 1999; Jugloff et al., 2000). A short duration of FlaSh expression (using the tet on/off system, for example) can thus be used to limit its opportunity to co-assemble with native subunits to a small fraction of the total pool, thus minimizing the electrophysiological impact. We are currently exploring these possibilities experimentally.

Mechanism of the fluorescence report

FlaSh undergoes three distinct kinetic phases of fluorescence change: an early phase on the time scale of channel opening, and intermediate and late phases that are on the time scale of slow inactivation. The three fluorescence phases are seen both in the conducting channel and in the mutant W434F channel, whose slow inactivation gate is locked shut and which consequently does not conduct ions, indicating that the fluorescence response of GFP does not depend on ion flux through the pore. Nor does the FlaSh fluorescence report appear to reflect changes in cellular ions, such as in Cl^- or protons (pH), that could occur with a voltage change, and to which GFP has demonstrated sensitivity, because the fluorescence response of FlaSh saturates at positive and negative voltages while the driving force for transmembrane ion flux and charge on the membrane do not. Instead, the fluorescence depends on channel gating. This was shown first from the correspondence between the voltage dependence of channel gating and FlaSh fluorescence (Siegel and Isacoff, 1997), and reinforced here from the effect of the L366A *Shaker* mutation that shifts in the negative direction both the voltage dependence of channel gating and FlaSh fluorescence. In sum, GFP inserted near the internal end of the *Shaker* channel S6 appears to change fluorescence because it senses three of the rearrangements of the channel that occur sequentially in response to membrane depolarization.

We find that the relative sensitivity of GFP to each of the channel motions depends on which GFP variant is used. While the intermediate component is most prominent in wtGFP, ecliptic GFP only has an early component and practically all of the YFP response is during the late component, with the others being more evenly mixed. Why is there such variety in the degree of sensitivity of the GFP variants to the different channel rearrangements? We consider two general mechanisms that could account for the responsiveness of GFP fluorescence to the channel rearrangements: 1) movement that changes interaction between GFPs on different subunits, and 2) mechanical deformation of GFP or changes in chromophore environment. The first of these mechanisms appears to contribute to the early phase of the fluorescence response. This insight comes from the observation that the early phase involves a decreased FRET in channels composed of mixed subunits of FlaSh (CFP) and FlaSh (YFP), indicating either an increase in distance or a change in relative dipole angle between CFP on one subunit and YFP on another. Such relative motion between subunits would be expected to decrease quenching previously documented for wtGFP-wtGFP or GFPuv-GFPuv interaction (De Angelis et al., 1998; Clonetech PT2020-1). Indeed, FlaSh (wtGFP) and FlaSh (GFPuv) both have an early phase that makes them brighter, consistent with the predicted dequenching. The expression and fluorometry of

linked tetramers of FlaSh with only one GFP subunit should enable us to determine this mechanism more clearly.

Unlike the early phase of fluorescence change, we have no indication that the intermediate or late phases depend on GFP-GFP interaction. We therefore provisionally consider that they reflect either a change in local environment due to structural rearrangements of the channel or mechanical deformation of GFP. The different GFPs differ in the relative sensitivity to these channel rearrangements, and in the relative brightness of the channel states. It is possible that structural rearrangements transmitted from the channel to GFP change the relative stability of different spectral states of GFP that have been documented for GFP (Heim et al., 1994; Tsien, 1998). The different states of GFP include multiple fluorescent states with distinct wavelengths of excitation and emission, and dark states, which are nonfluorescent (Brejc et al., 1997; Creemers et al., 1999; Schwille et al., 2000; Weber et al., 1999; Garcia-Parajo et al., 2000). The character and stability of the GFP states differ between different GFP variants due to the structure and chemical environment of the chromophore (Tsien, 1998; Brejc et al., 1997; Wachter et al., 1998; Elsliger et al., 1999; Bell et al., 2000). This may explain the difference we found in polarity of the ΔF and in the relative sensitivities to the different channel rearrangements. GFP inter-converts rapidly between its different states (Schwille et al., 2000; García-Parajo et al., 2000; Haupts et al., 1998; Volkmer et al., 2000). It is possible that the inter-conversion rates are sensitive to the change in GFP environment or to mechanical stress on GFP induced by the structural rearrangements of the channel.

The opposite polarity of the ΔF in FlaSh (eGFP) when excited at shorter wavelengths versus longer wavelengths is consistent with changes in the relative amplitude of the shorter wavelength excitation shoulder and longer wavelength excitation peak. Because the other GFPs do not change their direction of fluorescence response with excitation at other wavelengths, they may represent changes in the relative stability of fluorescent and dark states (e.g., YFP may increase brightness due to a decreased stability of a dark state).

Optimizing the fluorescence response

The new variant GFP versions of FlaSh all have improved folding at 37°C, a necessity for adapting FlaSh for use in mammalian preparations. In addition, longer-wavelength versions are expected to reduce background autofluorescence. Furthermore, the differences in spectra between the variants should make it possible to target different colored sensors to different cell types to enable the synchronous measure of activity from multiple subpopulations of intermingled cells in the same neural circuit.

One additional advantage is the ability to expand the optical readout from changes in fluorescence intensity over a single narrow band of wavelengths to dual wavelength measurements based on spectral shifts in FlaSh (eGFP) or on FRET between FlaSh (CFP) and FlaSh (YFP). A dual wavelength measure affords the advantage of eliminating the problem of movement artifact or changes in reporter levels in the optical slice, and can augment the fractional signal change.

Tuning kinetics

FlaSh is not a typical fluorescent voltage probe. Traditional "fast" voltage-sensitive dyes have been designed to respond in microseconds and linearly to membrane potential (Cohen and Lesher, 1986; Gross and Loew, 1989; Gonzalez and Tsien, 1997). In contrast, FlaSh (wtGFP) responds nonlinearly in the tens of milliseconds range. Although the response rate is slow, short impulses produce substantial responses. The responses are stretched-out stereotypical fluorescent transients.

Changing the GFP to Ecliptic GFP, which we find to be only sensitive to the early component of channel gating, made FlaSh much faster, with the ON response limited to the duration of the depolarization. This acceleration of the FlaSh response increases the rate at which FlaSh can follow multiple action potentials. Another fast FlaSh was achieved by removing the N-terminal inactivation ball from the channel, although this acts at the expense of a reduction in the size of the impulse response. The significance of this is that ball removal can be used with any of the GFPs, thus providing alternate colors of "fast" indicator. The success of the kinetic adjustment by channel mutation indicates that other kinds of mutations already described in the literature to alter the rates of specific gating rearrangements can be used to rationally tune FlaSh kinetics.

Tuning dynamic range

Given the narrow voltage range over which *Shaker* channels gate, and FlaSh modulates its brightness, it is clear that some voltage signals will be reported more efficiently, while others may be missed altogether. We examined the response of FlaSh to physiologically realistic voltage waves driven by ionic currents through several distinct ion channel/receptor systems in several cell types of the salamander retina. We found that FlaSh fluorescence followed with different degrees of accuracy the electrical activity of the different signals when the native activity was applied via the voltage clamp to the oocytes. The closest approximation was of slower components of the voltage signal for cells whose voltage range coincides with that of the wild-type *Shaker* channel. The FlaSh responses to faster components of the voltage waves were distorted demanding faster versions of FlaSh, which may be made through the use of channel mutations that accelerate gating.

FlaSh did not capture the response of wide-field amacrine cells because the main response of these cell types occurs outside of the voltage range of wild-type *Shaker*. We adjusted the voltage range of FlaSh with one of many mutations that have been documented to shift voltage dependence of *Shaker* gating. The L366A mutant version of FlaSh operated, as predicted, at more negative voltages than the original FlaSh, and very much augmented the optical detection of the wide-field amacrine cell voltage wave. FlaSh (L366A) is well-suited to follow synaptic activity in most cells, while wild-type FlaSh is well-suited to detecting depolarizations to voltages more positive than −40 mV, such as action potentials.

In summary, we have modified the kinetics, dynamic range, and color of our optical voltage-sensor FlaSh. By modifying the GFP reporter we have produced sensors with improved folding at 37°C, making it suitable for use in mammalian preparations, and introduced sensors with distinct spectra and distinct kinetics. We also expanded our optical readout from single-wavelength fluorescence intensity changes to dual wavelength measurements based on spectral shifts and FRET, thus providing ratiometric readouts. These changes were "rational" in the terms of our choice of reporter color and in the production of FRET partners. The kinetics, direction of fluorescence change, and presence of ratiometric measure were not predicted. However, mutations of the channel were entirely rational, with mutations known to alter gating kinetics and voltage dependence yielding FlaSh variants with the predicted properties. The versions of FlaSh can now be optimized for the detection of action potentials, on one hand, or synaptic potentials, on the other, and can be adapted for cell types with distinct voltage ranges of operation.

We thank Scott Fraser, Henry Lester, Carver Mead, Gilles Laurent, Norman Davidson, Sanjoy Mahajan, John Ngai, and members of the Isacoff lab for helpful discussions.

This research was supported by the Office for Naval Research funding to Molecular Design Institute-II, a Laboratory-Directed Research Award from the Lawrence Berkeley National Laboratory, Howard Hughes predoctoral fellowships to G.G. and M.S.S., and University of California Biotechnology Research and Education Program training grant support for B.R.

REFERENCES

Ataka, K., and V. A. Pieribone. 2002. A genetically targetable fluorescent probe of channel gating with rapid kinetics. *Biophys. J.* 82:509–516.

Baird, G. S., D. A. Zacharias, and R. Y. Tsien. 1999. Circular permutation and receptor insertion within green fluorescent proteins. *Proc. Natl. Acad. Sci. U.S.A.* 96:11241–11246.

Baukrowitz, T., and G. Yellen. 1996. Two functionally distinct subsites for the binding of internal blockers to the pore of voltage-activated K^+ channels. *Proc. Natl. Acad. Sci. U.S.A.* 93:13357–13361.

Bell, A. F., X. He, R. M. Wachter, and P. J. Tonge. 2000. Probing the ground state structure of the green fluorescent protein chromophore using Raman spectroscopy. *Biochemistry.* 39:4423–4431.

Brejc, K., T. K. Sixma, A. Kitts, S. R. Kain, R. Y. Tsien, M. Ormo, and S. J. Remington. 1997. Structural basis for dual excitation and photoisomerization of the *Aequorea victoria* green fluorescent protein. *Proc. Natl. Acad. Sci. U.S.A.* 94:2306–2311.

Clonetech Living Colors User Manual PT2020–1 (PR94845), 1999. Clonetech.

Cohen, L. B., and S. Lesher. 1986. Optical monitoring of membrane potential: methods of multisite optical measurement. *Soc. Gen. Physiol. Ser.* 40:71–99.

Crameri, A., E. A. Whitehorn, E. Tate, and W. P. Stemmer. 1996. Improved green fluorescent protein by molecular evolution using DNA shuffling. *Nat. Biotech.* 14:315–319.

Creemers, T. M. H., A. J. Lock, V. Subramaniam, T. M. Jovin, and S. Völker. 1999. Three photoconvertible forms of green fluorescent protein identified by spectral hole-burning. *Nat. Struct. Biol.* 6:557–560.

De Angelis, D. A., G. Miesenbock, B. V. Zemelman, and J. E. Rothman. 1998. PRIM: proximity imaging of green fluorescent protein-tagged polypeptides. *Proc. Natl. Acad. Sci. U.S.A.* 95:12312–12316.

Elsliger, M.-A., R. M. Wachter, G. T. Hanson, K. Kallio, and S. J. Remington. 1999. Structural and spectral response of green fluorescent protein variants to changes in pH. *Biochemistry.* 38:5296–5301.

Garcia-Parajo, M. F., G. M. J. Segers-Nolten, J.-A. Veerman, J. Greve, and N. F. van Hulst. 2000. Real time light-driven dynamics of the fluorescence emission in individual green fluorescent proteins. *Biophys. J.* 78:384*a*. (Abstr.).

Gonzalez, J. E., and R. Y. Tsien. 1997. Improved indicators of cell membrane potential that use fluorescence resonance energy transfer. *Chem. Biol.* 4:269–277.

Gross, D., and L. M. Loew. 1989. Fluorescent indicators of membrane potential: microspectrofluorometry and imaging. *Methods Cell Biol.* 30:193–218.

Haupts, U., S. Maiti, P. Schwille, and W. W. Webb. 1998. Dynamics of fluorescence fluctuations in green fluorescent protein observed by fluorescence correlation spectroscopy. *Proc. Natl. Acad. Sci. U.S.A.* 95: 13573–13578.

Heim, R., D. C. Prasher, and R. Y. Tsien. 1994. Wavelength mutations and posttranslational autoxidation of green fluorescent protein. *Proc. Natl. Acad. Sci. U.S.A.* 91:12501–12504.

Heim, R., and R. Y. Tsien. 1996. Engineering green fluorescent protein for improved brightness, longer wavelengths and fluorescence resonance energy transfer. *Curr. Biol.* 6:178–182.

Hoshi, T., W. N. Zagotta, and R. W. Aldrich. 1990. Biophysical and molecular mechanisms of *Shaker* potassium channel inactivation. *Science.* 250:533–538.

Isacoff, E. Y., Y. Jan, and L. Y. Jan. 1990. Evidence for the formation of heteromultimeric potassium channels in *Xenopus* oocytes. *Nature.* 345: 530–534.

Jayaraman, S., P. Haggie, R. M. Wachter, S. J. Remington, and A. S. Verkman. 2000. Mechanism and cellular applications of a green fluorescent protein-based halide sensor. *J. Biol. Chem.* 275:6047–6050.

Jiang, Y., A. Lee, J. Chen, M. Cadene, B. T. Chairt, and R. MacKinnon. 2002. The open pore conformation of potassium channels. *Nature*. 417:523–526.

Jugloff, D. G. M., R. Khanna, L. C. Schilchter, and O. T. Jones. 2000. Internalization of the Kv1.4 potassium channel is suppressed by clustering interactions with PSD-95. *J. Biol. Chem.* 275:1357–1364.

Kneen, M., J. Farinas, Y. Li, and A. S. Verkman. 1998. Green fluorescent protein as a noninvasive intracellular pH indicator. *Biophys. J.* 74: 1591–1599.

Liman, E. R., J. Tytgat, and P. Hess. 1992. Subunit stoichiometry of a mammalian K^+ channel determined by construction of multimeric cDNAs. *Neuron.* 9:861–871.

Liu, Y., M. Holmgren, M. E. Jurman, and G. Yellen. 1997. Gated access to the pore of a voltage-dependent K^+ channel. *Neuron.* 19:175–184.

Llopis, J., J. M. McCaffery, A. Miyawaki, M. G. Farquhar, and R. Y. Tsien. 1998. Measurement of cytosolic, mitochondrial, and Golgi pH in single living cells with green fluorescent proteins. *Proc. Natl. Acad. Sci. U.S.A.* 95:6803–6808.

Lopez, G. A., Y. Jan, and L. Y. Jan. 1991. Hydrophobic substitution mutations in the S4 sequence alter voltage-dependent gating in *Shaker* K^+ channels. *Neuron.* 7:327–336.

Mannuzzu, L. M., M. M. Moronne, and E. I. Isacoff. 1996. Direct physical measure of conformational rearrangement underlying potassium channel gating. *Science.* 271:213–216.

Miesenbock, G., D. A. De Angelis. and J. E. Rothman. 1998. Visualizing secretion and synaptic transmission with pH-sensitive green fluorescent proteins. *Nature.* 394:192–195.

Miyawaki, A., O. Griesbeck, R. Heim, and R. Y. Tsien. 1999. Dynamic and quantitative Ca^{2+} measurements using improved cameleons. *Proc. Natl. Acad. Sci. U.S.A.* 96:2135–2140.

Miyawaki, A., J. Llopis, R. Heim, J. M. McCaffery, J. A. Adams, M. Ikura, and R. Y. Tsien. 1997. Fluorescent indicators for Ca^{2+} based on green fluorescent proteins and calmodulin. *Nature.* 388:882–887.

Mizuno, H., A. Sawano, P. Eli, H. Hama, and A. Miyawaki. 2001. Red fluorescent protein from *Discosoma* as a fusion tag and a partner for fluorescence resonance energy transfer. *Biochemistry.* 40:2502–2510.

Nagai, Y., M. Miyazaki, R. Aoki, T. Zama, S. Inouye, K. Hirose, M. Iino, and M. Hagiwara. 2000. A fluorescent indicator for visualizing cAMP-induced phosphorylation in vivo. *Nat. Biotechnol.* 18:313–316.

Okabe, S., H.-D. Kim, A. Miwa, T. Kuriu, and H. Okado. 1999. Continual remodeling of postsynaptic density and its regulation by synaptic activity. *Nat. Neurosci.* 2:804–811.

Ormo, M., A. B. Cubitt, K. Kallio, L. A. Gross, R. Y. Tsien, and S. J. Remington. 1996. Crystal structure of the *Aequorea victoria* green fluorescent protein. *Science.* 273:1392–1395.

Patterson, G. H., S. M. Knobel, W. D. Sharif, S. R. Kain, and D. Piston. 1997. Use of the green fluorescent protein and its mutants in quantitative fluorescence microscopy. *Biophys. J.* 73:2782–2790.

Pearce, L. L., R. E. Gandley, W. Han, K. Wasserloos, M. Stitt, A. J. Kanai, M. K. McLaughlin, B. R. Pitt, and E. S. Levitan. 2000. Role of metallothionein in nitric oxide signaling as revealed by a green fluorescent fusion protein. *Proc. Natl. Acad. Sci. U.S.A.* 97:477–482.

Perozo, E., R. MacKinnon, F. Bezanilla, and E. Stefani. 1993. Gating currents from a nonconducting mutant reveal open-closed conformation in *Shaker* K^+ channels. *Neuron.* 11:353–358.

Romoser, V. A., P. M. Hinkle, and A. Persechini. 1997. Detection in living cells of Ca^{2+}-dependent changes in the fluorescence emission of an indicator composed of two green fluorescent protein variants linked by a calmodulin-binding sequence: a new class of fluorescent indicators. *J. Biol. Chem.* 272:13270–13274.

Roska, B., E. Nemeth, and F. S. Werblin. 1998. Response to change is facilitated by a three-neuron disinhibitory pathway in the tiger salamander retina. *J. Neurosci.* 18:3451–3459.

Sakai, R., V. Repunte-Canonigo, C. D. Raj, and T. Knopfel. 2001. Design and characterization of a DNA-encoded, voltage-sensitive fluorescent protein. *Eur. J. Neurosci.* 13:2314–2318.

Schoppa, N. E., and F. J. Sigworth. 1998. Activation of *Shaker* potassium channels. I. Characterization of voltage-dependent transitions. *J. Gen. Physiol.* 111:271–294.

Schwille, P., S. Kummer, A. A. Heikal, W. E. Moerner, and W. W. Webb. 2000. Fluorescence correlation spectroscopy reveals fast optical excitation-driven intramolecular dynamics of yellow fluorescent proteins. *Proc. Natl. Acad. Sci. U.S.A.* 97:151–156.

Siegel, M. S., and E. Y. Isacoff. 1997. A genetically encoded optical probe of membrane voltage. *Neuron.* 19:735–741.

Tsien, R. Y. 1998. The green fluorescent protein. *Annu. Rev. Biochem.* 67:509–544.

Tytgat, J., K. Nakazawa, A. Gross, and P. Hess. 1993. Pursuing the voltage sensor of a voltage-gated mammalian potassium channel. *J. Biol. Chem.* 268:23777–23779.

Volkmer, A., V. Subramaniam, D. J. Birch, and T. M. Jovin. 2000. One- and two-photon excited fluorescence lifetimes and anisotropy decays of green fluorescent proteins. *Biophys. J.* 78:1589–1598.

Wachter, R. M., M.-A. Elsliger, K. Kallio, G. T. Hanson, and S. J. Remington. 1998. Structural basis of spectral shifts in the yellow-emission variants of green fluorescent protein. *Structure.* 6:1267–1277.

Weber, W., V. Helms, J. A. McCammon, and P. W. Langhoff. 1999. Shedding light on the dark and weakly fluorescent states of green fluorescent proteins. *Proc. Natl. Acad. Sci. U.S.A.* 96:6177–6182.

Yang, Y., Y. Yan, and F. J. Sigworth. 1997. How does the W434F mutation block current in *Shaker* potassium channels? *J. Gen. Physiol.* 109: 779–789.